JOURNAL OF GEOPHYSICAL RESEARCH, VOL. 111, A07S06, doi:10.1029/2005JA011434, 2006

Heliospheric ion energization due to emerging CME shocks

I. Roth[1] and S. D. Bale[1]

Received 16 September 2005; revised 6 April 2006; accepted 2 May 2006; published 15 July 2006.

[1] Formation of inhomogeneous electromagnetic structures with gradients in magnetic field and intrinsic electric fields is commonly observed in magnetized plasmas. Heliospheric plasmas are susceptible to formation of localized, supersonically propagating electromagnetic inhomogeneities. Coronal relaxation may result in an emergence close to solar surface of a shock wave which traverses significant parts of the heliosphere. Shocks of solar origin may accelerate ions to high energies, and some of these ions can be trapped in quasi-stable orbits of planetary magnetospheres. The observationally deduced ion acceleration close to the Sun, at low Mach numbers and low turbulence levels, poses a dilemma regarding the energization mechanism. When the magnetic ramp of an obliquely propagating electromagnetic substructure narrows to a size of a fraction of ion skin depth, as conjectured during merging of successively propagating shocks, the trajectories of some ions exhibit strongly nonadiabatic characteristics. Subset of ions is energized while surfing along the shock due to the combined forces of magnetic fields and cross-shock electric potential gradient, forming a high-energy tail. This tail may be additionally accelerated after traversing the shock multiple times as a result of scattering and reflection due to Alfvenic wave diffusion. We follow the orbits of seed ions in a presence of a stationary, fluid-based, self-consistent model, and investigate their behavior for a variety of plasma parameters and geometries. The results indicate that (1) the energization of ions for low Mach numbers, as observed for emerging shocks close to the Sun, depends crucially on the narrowness of the electromagnetic structures, (2) the sufficiently narrow heliospheric structure can energize thermal protons and a subset of rare ions which were enriched due to impulsive coronal processes, (3) the energization is sensitive to the pitch angle of the seed population, indicating dependence on the geometry of the shock-plasma flow system, and (4) the preacceleration by surfing mechanism is a prerequisite for an additional energization due to diffusive shock acceleration. We conclude that the best configuration for an effective acceleration due to an emerging shock at small heliocentric distances and low Mach number consists of a narrow electromagnetic substructure which energizes heliospheric thermal protons directly from their thermal level, as well as trace elements which enrich the seed population due to previous coronal processes. The narrowness of the shock or its substructure and the surfing mechanism may help in explaining the observed energization when other mechanisms become inefficient due to an insufficient level of the turbulence. The energetic ion populations may have a direct profound impact on human space exploration.

Citation: Roth, I., and S. D. Bale (2006), Heliospheric ion energization due to emerging CME shocks, *J. Geophys. Res.*, *111*, A07S06, doi:10.1029/2005JA011434.

1. Introduction

[2] Heliospheric acceleration of thermal populations to high energies (1–100 MeV) due to interplanetary, propagating shocks, is of importance (1) in the investigation of basic interaction of plasma with naturally formed, nonlinear electromagnetic structures, and (2) in an analysis of intense solar and heliospheric perturbations on the terrestrial magnetic configuration which renders the solar energetic particles (SEPs) access and allows their trapping at the quasi-stable magnetospheric orbits. Shock induced trapping of solar-origin protons and heavy ions on terrestrial magnetic field lines was demonstrated by Earth-orbiting spacecraft when new hydrogen and Fe stable belts were formed impulsively over timescales of tens of minutes to hours [*Blake et al.*, 1992; *Hudson et al.*, 1998; *Lorentzen et al.*, 2002]. The formation of electromagnetic shocks and the resulting heliospheric emergence and magnetospheric trapping of energetic populations constitute an important part of the Sun-Earth connection

[1]Space Sciences Laboratory, University of California, Berkeley, Berkeley, California, USA.

0148-0227/06/2005JA011434$09.00

research theme, both being crucial in our understanding of the intense terrestrial perturbations and in assessing the risk to human activity in space.

[3] The propagating heliospheric shocks are formed due to physical processes which originate in the magnetized solar corona. The reconfiguration of twisted coronal field lines may result in a supersonic expulsion of a large blob of plasma (10^{15}–10^{16} g) into the interplanetary medium in the form of coronal mass ejection (CME), which carries a shock at its leading edge [e.g., *Kahler*, 1992; *Reames*, 1999]. This electromagnetic shock propagates from the Sun over a significant fraction of the heliosphere, energizing the ambient plasma along its path [e.g., *Reames and Tylka*, 2002; *Tylka et al.*, 2005]. Since the free energy is embedded in the twisted coronal field, the CMEs are formed mainly during the period of high solar activity, with a lower occurrence in the declining phase.

[4] Shock energization depends on the upstream plasma parameters, on the seed population, on the propagation speed (Mach number) of the shock, and on its internal structure. The seed plasma population is made up of solar wind plasma (''cosmic'' abundances) with modifications due to (1) enhancement of elements with a low first ionization potential in fast solar wind (SW) stream, which originate in coronal holes [*Reames et al.*, 1991]; (2) enrichment of interplanetary plasma due to coronal processes of a set of rare elements and isotopes, mainly ^{3}He, Fe group, and ultraheavy elements at the Xe and Kr groups [*Reames*, 2000; *Mason et al.*, 2004], and (3) addition of ions which originate as a neutral interstellar or interplanetary dust source which got ionized and picked up by the solar wind [e.g., *Gloeckler et al.*, 2000].

[5] The acceleration processes by shocks has been investigated over several decades. In the astrophysical context it is widely believed that cosmic rays are energized due to first-order Fermi mechanism (diffusive acceleration) at the strong shock waves of supernova remnants [*Krymsky*, 1977; *Axford*, 1981; *Drury*, 1983; *Blandford and Eichler*, 1987]. Many theoretical approaches included particle interaction with hydrodynamic shock front where the magnetic field plays only a secondary role, determining the elastic scattering off the magnetic irregularities and the values of the spatial diffusion coefficients [e.g., *Drury*, 1983]. The analysis used a diffusion-convection (cosmic ray) equation for an isotropic distribution function with (1) an adjusted spatial coefficient, (2) model deceleration of the bulk motion, and (3) neglect of the momentum diffusion [*Duffy et al.*, 1994; *Ellison and Reynolds*, 1991; *Zank et al.*, 2000] or a focused transport equation [e.g., *Lee*, 2005], which implements a quasilinear momentum diffusion operator. Inclusion of explicit magnetic wave fields assigns the Alfven waves as a source of the turbulence required for the diffusive shock acceleration and relates the spatial diffusion (owing to the stationary or time dependent magnetic fluctuations) to the inverse of the quasilinear pitch angle operator. In this process, repeated scattering and reflection by waves excited by previously accelerated particles in the extended region of the shock, and the subsequent multiple crossing of ions through the shock, experiencing the compression between the upstream and downstream flows (Fermi process) or intermittent drift along the convection field (shock-drift), allows the particles to acquire energy of many MeV/nucleon before being ejected sufficiently far from the shock and transported to the observing satellite. Alfven waves which propagate in both directions along and opposite to the magnetic field eliminate the problematic pitch angle gap in the quasilinear operator allowing a smooth scattering of the particles which then can reenter the shock. Additionally, it was shown that in a presence of a general wave spectrum the momentum diffusion should be included in the basic cosmic ray equation [*Schlickeiser*, 1989]. However, in all these descriptions it has been assumed that the distribution function is rapidly isotropized in pitch angle and averaged over the gyrophase. Detailed measurements at the terrestrial bow shock and at the propagating heliospheric shocks, as well as numerous simulations [e.g., *Lembege et al.*, 2003] showed that both assumptions regarding fast pitch angle isotropization and gyrotropic interaction may not always be valid. Trajectories of the accelerated particles which consist only of a small initial subset of the ion distribution, with an insignificant pressure to affect the shock structure, may violate the above assumptions. Therefore ion energization may depend on its pitch angle and gyrophase at the entry into the shock, i.e., on the initial conditions and the flow-shock configuration, and full particle trajectories may be required to obtain a valid description of the energization process.

[6] Figure 1 shows the Mach number (propagation speed normalized by a local Alfven velocity) as a function of the heliocentric distance, based on a model of heliospheric magnetic field and density, for varying shock propagation velocities. Since the Alfven velocity reaches a maximum value in the proximity to solar surface and then decreases slowly with the heliocentric distance, reverse applies to the Mach number. One observes that in the proximity to Sun, at 5–10 solar radii R_s, for a wide range of propagation speeds, the shock is barely supersonic, while beyond a distance of 1 AU the Mach number of a CME which emerges from the corona covers a range of Mach numbers. Taking into account the differential speed with respect to the solar wind and due to the slow-down in the shock speed as a result of the background drag, most of the observed interplanetary shocks reach values of Mach 1.5–5, with an extension of the distribution all the way to Mach 15; multisatellite data indicate a decrease in CME speed by a factor of more than 2 at the Jovian orbit, while observations related to the Bastille Day (2000) event at WIND (1 AU) and Voyager (63 AU) measured the decrease in the speed jump due to CME from 400 km/s to 60 km/s [*Wang et al.*, 2001]. The structure of the shock depends on the external plasma parameters (β, density, obliqueness, Mach number), which determine the relations between the upstream and downstream quantities. However, important features of the internal structure depend on the spatial dependence of the electromagnetic fields in the transition region and on its width which is measured in units of the gyroradius ρ or ion skin depth c/ω_i, where c denotes the speed of light and ω_i is the ion plasma frequency; using the heliospheric model and assuming a density of 5 ions/cc at 1 AU, the ion skin depth becomes 100 km at 1 AU, 10 km at 20 $R_s \sim 0.1$ AU, and 500 km at 5 AU. Similarly, the ratio of ion gyrofrequency to ion plasma frequency is approximately 0.0002 at 1 AU, 0.002 at 20 R_s, and 0.00008 at 5 AU. The changing values of the Mach number, the gyro/plasma frequency ratio, and

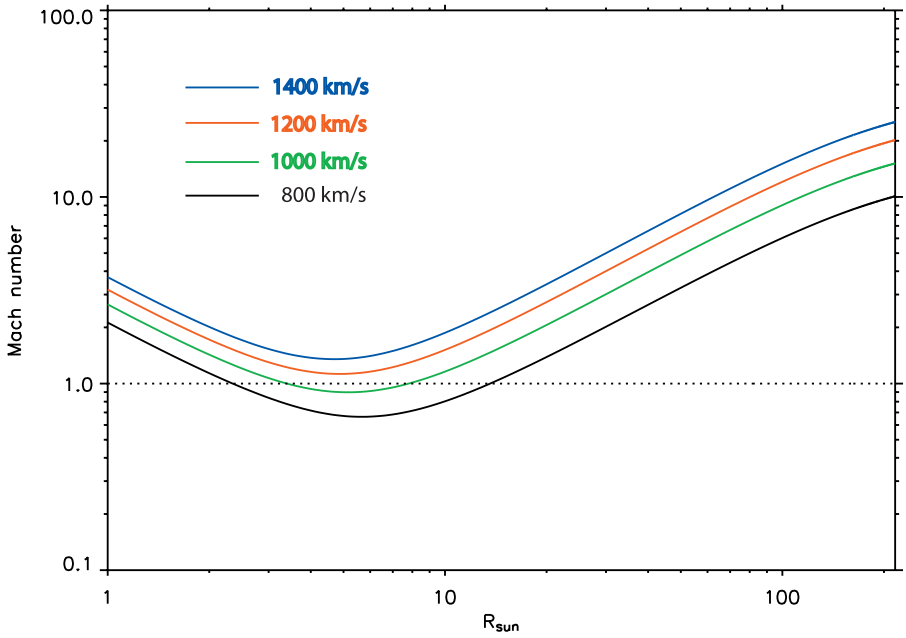

Figure 1. Dependence of Alfvenic Mach number on the heliocentric distance for several propagation speeds.

skin depth impose specific requirements on the shocks structure for efficient acceleration processes.

[7] Observations of CME shocks [e.g., *Reames*, 1999; *Reames et al.*, 2000, 2001; *Tylka et al.*, 2002] indicate that the main enhancement of fluxes of energetic ions, including heavy ions (Fe) with high charge state occurs often at very low heliocentric distances, at few solar radii, where even for the fastest propagating shocks the magnetic Mach number is relatively low (below 2). Additionally, there may exist an observational correlation between the most energetic ion events and merging of multiple interacting CMEs with vastly different speeds [*Gopalswamy et al.*, 2002]. Similarly, the most intense events (rogue events) are well correlated to an observation of two (converging) CME shocks [*Kallenrode and Cliver*, 2001a]. Formation of successive propagating shocks is an observationally documented effect. In many instances strong reconfiguration of coronal field lines with an ejection of CME destabilizes an adjacent region or creates conditions at the same active region susceptible to reformation of a magnetically unstable configuration, allowing successive emergence of "sympathetic" or homologous CMEs, respectively [e.g., *Cheng et al.*, 2005]. The intense interaction between propagating shocks may plausibly deform the CME into narrow inhomogeneous substructure(s) which, as will be shown later, may accelerate a subset of ions to very high energies, even without the turbulence required by the Fermi process. Analogously, solar rotation and the spatial variability in the solar wind velocity allows the fast solar wind stream which emanates from the magnetically unconstrained low density coronal holes, to interact with a slower, higher-density solar wind which is emitted from the vicinity of magnetized coronal loops, to form successive compression and rarefaction regions. For a quasi-stationary pattern of flow this interaction, which usually takes place effectively at large heliocentric distances (beyond 1 AU), forms one of the most prevalent, repetitive heliospheric Corrotating Interaction Regions (CIR), where the leading and trailing edges form the forward and reverse shocks, respectively, which were shown as source of ion acceleration [e.g., *McDonald et al.*, 1976; *Hundhausen and Gosling*, 1976; *Fisk and Lee*, 1980]. In both circumstances an interaction between two stable entities may form a new inhomogeneous configuration.

[8] In the solar vicinity a propagating shock with a low Mach number (and a resulting low turbulence level) becomes inefficient in scattering the ions multiple times back to the shock as required by the diffusive shock acceleration process. Because of this drawback, we conjecture that the configuration which allows for the most efficient acceleration in the solar vicinity at low Mach numbers forms a (set of) narrow sheath(s), presumably due to merging of two or more disparate CMEs with differential velocities. This (sub)structure will allow the ions to surf along its surface, energizing a seed population which consist of the bulk or suprathermal solar wind plasma with contamination due to previously enriched solar trace elements.

[9] In this paper we discuss the kinetic behavior of seed ions interacting with a stationary, fluid-based, shock model, comprising of cross-shock electric field and rotated magnetic field. We focus primarily on the acceleration process in the solar vicinity. Section 2 presents the shock model based on the experimental and numerical input for its structure. Section 3 investigates the intricate trajectories in the presence of the shock model with inclusion of waves and presents the resulting distribution functions for energetic ions of solar wind plasma and for a representative of minority trace elements, and section 4 summarizes the finding in the general view of heliospheric ion acceleration.

2. Description of the Shock Model

[10] Supersonically propagating interplanetary shock develops a unique inhomogeneous and highly nonlinear

structure. This structure consists of a layer in which microscopic dissipation processes allow for an irreversible changes in macroscopic quantities. Electromagnetic shocks are formed due to a steepening of a naturally excited wave which grows beyond the linear stage and dissipates energy in a narrow sheath. As a result, a structure, which moves supersonically with respect to the ambient plasma, is formed with a ramp in magnetic field, plasma bulk velocity, density, and other thermodynamic quantities. The up-stream and down-stream flow regions of the shock consist of different thermodynamic states which are linked via a dissipative layer. The disparate values of the ion and electron gyroradii and the steepening in the magnetic structure causes diversion in the trajectories of these particles. This separation of trajectories forms the necessary current which supports the magnetic field inhomogeneity; it also violates the MHD approximation, requiring kinetic description of the ensuing plasma. One way in which the frozen-in condition can be violated is via a large resistivity, which has been used by many researchers; it allows to implement successfully dissipation processes into large-scale models which are being developed for space weather analysis and prediction of terrestrial perturbations [e.g., *Mikic and Linker*, 1994]: however, this approach averages and isotropizes the behavior of plasma particles, whose trajectories depend on the details of the sheath layer, where the effect of Hall term, pressure gradients and electron inertia are often more important than the resistivity. Additionally, the mesh size of the numerical global models grossly overestimates the size of the magnetic ramp, which is crucial in the analysis of trajectories of a subset of ions which may form the high-energy tail. The diversion in the trajectories of ions and electrons causes also a small charge separation which forms the cross-shock electric field: this field balances the magnetic field and the thermal pressure forces. In an oblique shock the normal magnetic field component deflects the bulk flow, forming secondary drifts which require another component of magnetic field in the sheath region. The stationary self-consistent electromagnetic fields, with a narrow ramp may affect profoundly a subset of particle trajectories to form an energetic tail (e.g., *Balikhin and Gedalin* [1994], *Gedalin et al.* [1995], *Ball and Galloway* [1998] for electrons; *Zilbersher and Gedalin* [1997] for ions).

[11] The shock consists of a nonlinear, inhomogeneous electromagnetic structure which satisfies several conservation laws [e.g., *Papadopoulos*, 1985] and connects the variables on the upstream and downstream sides. However, the thickness of the compression region ramp is not determined by these conservation relations; it evolves self-consistently due to the dynamic interaction between two solar wind streams (CIR), between solar wind and magnetized body (bow shock), between multiple CME perturbations or when an intense CME traversing rapidly changing background plasma, and is regulated by the seed of interacting particles. This interaction is determined partly by the geometrical configuration of the shock versus solar wind or between two CMEs, and by the thermodynamic state of the upstream plasma. Therefore parametrization of the energization with respect to the geometry, thermodynamics, wave activity, and shock structure is important for a diagnostics of the propagating shock. On the basis of particle simulation results [e.g., *Scholer et al.*, 2003] and observational indications [*Gopalswamy et al.*, 2002], it is plausible to consider shock substructure with a narrow sheath, rotation of the magnetic field and a cross-structure electric field. This combination of fields may ''trap'' some ions along the structure surface and energize them due to the motional electric field.

[12] Since almost all of the observed heliospheric structures exhibit curvatures with very large-scale lengths (many tens of thousands of kilometers), one may assume in first-order that locally the shock is one-dimensional, i.e., the gradients are function of only one coordinate, x. From the self-consistency point of view it means that the acceleration processes take place on spatial scales much smaller than the curvature or ripples in the electromagnetic structure. Similarly, in order to implement the conservation laws which apply to stationary shock, one assumes that the timescale of crossing ions must be shorter than the time in which the shock modifies its structure. We believe that large-scale ripples will not have a significant effect on the energization process.

[13] In the case of a planar, stationary structure we construct a fluid-based configuration: the magnetic field upstream is given by $\mathbf{B} = [B_x, 0, B_{zo}]$, downstream by $\mathbf{B} = [B_x, 0, B_1]$, while in the ramp by $\mathbf{B} = [B_x, B_y(x), B_z(x)]$; an explicit form for the main component $B_z(x)$ is assigned in an approximate form obtained from time-averaged experimental observations with correction due to boundary relations; the other macroscopic quantities: density N, velocity V, and pressure P, are assigned unperturbed upstream values N_o, V_o, and P_o, respectively, and in the ramp region become functions of x, in consistency with the conservation laws. In a planar configuration B_x is unmodified across the shock and finite values of B_y are confined to the sheath. Downstream all the quantities relax to their asymptotic values. Depending on the shock configuration, we allow for an upstream oblique incidence of the plasma flow: $\mathbf{V} = [V_o, 0, V_{zo}]$, which may influence the kinetic interaction at the shock and the final energization. The self-consistent picture includes clearly wave activity and time-dependence of the shock ramp.

[14] From the stationary ion momentum equation and conservation of particle flux: $N(x)\,V(x) = N_o V_o$, one obtains the plasma flows in the shock ramp [*Tidman and Krall*, 1971]:

$$V_x(x) = V_o - \left[B_y{}^2(x) + B_z{}^2(x) - B_{zo}{}^2(x)\right] /8\pi M N_o V_o - [P(x) - P_o]/M N_o V_o \tag{1}$$

$$V_y(x) = [B_x/4\pi M N_o V_o]B_y \tag{2}$$

$$V_z(x) = V_{zo} + [B_x/4\pi M N_o V_o](B_z(x) - B_{zo}) \tag{3}$$

while Ohm's Law and $\nabla \times \mathbf{E} = 0$ give the additional ramp relations:

$$V_y(x)B_x - V_x(x)B_y(x) + (Mc/e)V_x(x)\partial_x V_z(x) + \left(c^2/4\pi\sigma\right)\partial_x B_y(x) = 0 \tag{4}$$

$$V_z(x)B_x - V_x(x)B_z(x) - (Mc/e)V_x(x)\partial_x V_y(x) + \left(c^2/4\pi\sigma\right)\partial_x B_z(x) = -V_o B_{zo} \tag{5}$$

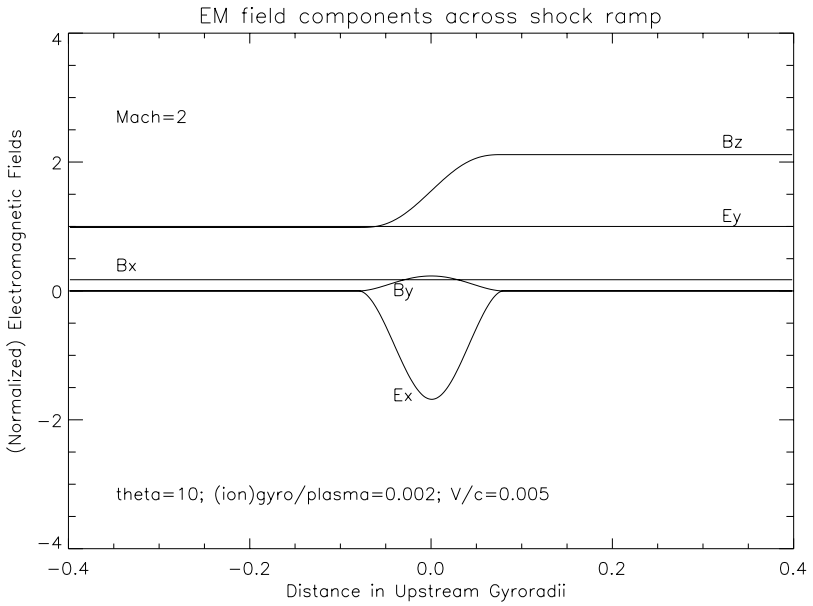

Figure 2. Components of the electromagnetic field across the shock. Shock parameters: $M_A = 2$, $\beta = 0.1$, $\theta = 10°$, $\nu = 0.01\ \Omega_i$. The width of the shock is ion skin depth: $2\delta = c/\omega_i$; ion gyro/plasma frequency ratio $\Omega_i/\omega_i = 0.002$. The gyrofrequency is related to the upstream bulk drift V and the gyroradius ρ: $\rho = V/\Omega_i$, $V/c = 0.005$.

with a conductivity $\sigma = Ne/M\nu$, where ν denotes the collisional frequency. Expressing the velocities V_i as functions of B_i, assuming a specific shape for the main magnetic field component B_z and correcting it according to the last equations, allows one to obtain the $B_y(x)$ component and the ambipolar cross-shock electric field: $\mathbf{E} = -\mathbf{V} \times \mathbf{B}/c + [(\nabla \times \mathbf{B}) \times \mathbf{B}]/(4\pi Ne) + (c/4\pi)\eta\nabla \times \mathbf{B} - \nabla P_e/Ne$ (with resistivity η), which for the chosen configuration with low β and η becomes $E_x = -V_y B_z/c + V_z B_y/c - \partial_x(B_z^2 + B_y^2)/8\pi Ne$. Additionally, in the frame of the shock, there exists a motional electric field E_y, which in a stationary configuration is constant across the shock ramp. One may observe that an important contribution to B_y as well as to E_x is proportional to the derivative of B_z. As an ansatz to form a self-consistent configuration of electromagnetic fields, we chose $B_z = B_{zo}\, 0.5\, [(r+1) + (r-1)\, g(x/\delta)]$, with $g(x) = 0.125\, [3x^5 - 10x^3 + 15x]$ in the shock region $-\delta < x < \delta$, and constant outside of the ramp such that the ramp function and its first derivative are continuous; it describes a ramp increasing by a factor r and extending over width 2δ. With an adiabatic or other pressure profile all the components of the magnetic and electric field are then uniquely determined.

[15] Figure 2 shows the electromagnetic field components across the shock for a set of shock parameters: plasma $\beta = 0.01$, the angle of the magnetic field off the perpendicular direction $\theta = 10°$, shock width $2\delta = c/\omega_i$, and ratio of ion gyro-to-plasma frequency = 0.002. The magnetic field components are normalized to the upstream magnetic field, while the electric field components are normalized to the electric field resulting from the transformation between the plasma and the shock frames. It is evident that an ion which crosses the shock may be significantly influenced by an increase and rotation in the magnetic field, as well as by the cross-shock potential and the motional electric field.

[16] The experimentally observed shock exhibits often temporal dependence and nonstationarity of its profile, while plasma simulations indicate self-reformation of the high Mach shock front on the scale of the ion gyrofrequency [*Scholer et al.*, 2003]. Regarding the diffusive acceleration process, the turbulence due to energized particles, mainly downstream, is crucial for the required scattering in Fermi acceleration. In order to simulate the additional turbulence on particle phase space motion, we impose on top of the shock model a spectrum of Alfven waves. This turbulent spectrum prescribes parallel and oblique waves which allow to interact with a variety of wave phase velocities; the two-dimensionally was shown as an intrinsic part of the spectrum in the heliosphere [*Roberts and Goldstein*, 1999] and in general cosmical plasma [*Goldreich and Sridhar*, 1995]. Specifically, we take a large number (200–500) of plane waves with a random propagation directions with respect to the local main component of the magnetic field for each wave, random phases and amplitudes drawn from a Kolmogoroff distribution proportional to P(k) with a cutoff Λ [*Giacalone and Ellison*, 2000]

$$P(k)dk = k^2 dk/(1.0 + k\Lambda)^{11/3} \tag{6}$$

and the integrated power of the waves at the shock location normalized to the ambient energy density given by σ_t, with a spatial decay rate of the turbulence power γ_L; since the flow downstream is more disturbed than upstream, we choose a larger decaying factor upstream (downstream turbulence more extended spatially). Comparison of trajectories with and without turbulence may indicate the importance of surfing along the shock as an acceleration process and as a prerequisite condition for the diffusive shock acceleration mechanism.

[17] In the frame of a stationary shock the values of up and down stream parameters are determined by the various fluxes which are conserved across a shock. The conservation of the mass, momentum, and energy flux results in a

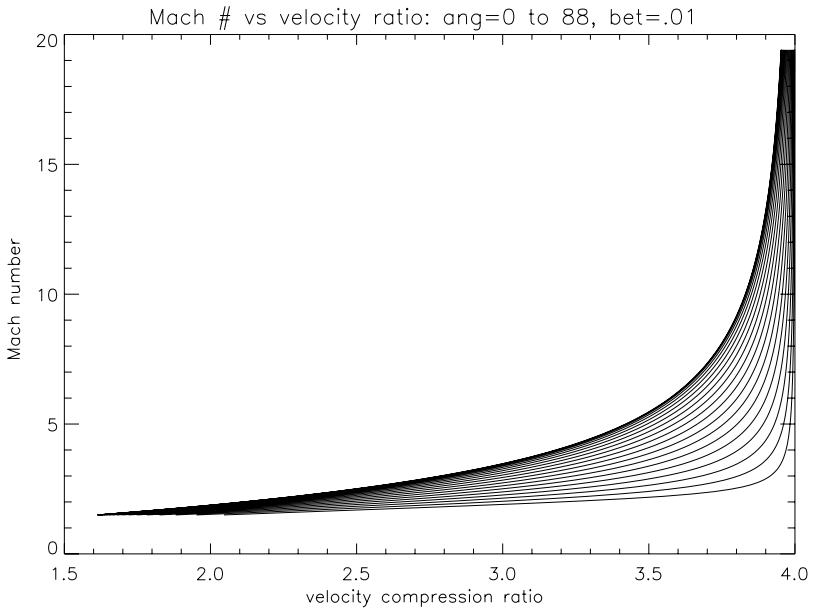

Figure 3. Solutions of R-H equations for $M_A - r$ with given β and ϕ and varying θ. Perpendicular shock is depicted as the leftmost graph.

specific relation between the Mach number M_A, plasma β, the angle between the upstream magnetic field and the shock surface θ, the angle of the impinging upstream solar wind with respect to shock normal ϕ, and the increase in the ramp value r, or equivalently in the compression ratio. Figure 3 shows the solution of the relation between M_A and r for given $\beta = 0.01$, $\phi = 0$ and varying θ between 0 and 90°. Here the adiabatic constant was taken as $\gamma = 5/3$. Varying γ or ϕ modifies the asymptotic values of the compression ratio. For nonrelativistic shocks without any feedback of the energized particles on the shock itself, the compression ratio is bounded by 4 and for low Mach number it is only slightly above unity, while a feedback contribution due to the accelerated population may increase the compression ratio to very high values [*Eichler*, 1984]. Figures 2 and 3, together with the time-dependent perturbations with power given by equation (6), constitute the configuration into which the seed particles are injected.

3. Numerical Simulation of Shock-Crossing Ions

[18] In order to analyze the effect of the propagating shock on the trajectories of the ions, we employ the electromagnetic structure as described in the model section (Figure 2) for given parameters of the upstream plasma and Mach number (Figure 3), with or without electromagnetic wave perturbations. We choose a reference frame of the (propagating) structure and follow representative ions in phase space to discern the changes in their orbits with different initial and varying external conditions. For each particle we propagate in time a six-dimensional vector which describes the phase space coordinates of the particle: $\mathbf{X} = (x, y, z, v_x, v_y, v_z)$. The set of the coupled equations

$$\dot{\mathbf{X}} = \mathbf{G}(\mathbf{X}) \tag{7}$$

where $\mathbf{G}$ describes the prescribed, static or time-dependent electromagnetic fields, is solved with an adaptive time step. In the upstream domain the shock normal is chosen along the x coordinate, while the oblique magnetic field is rotated such that $\mathbf{B} = [B_o \sin\theta, 0, B_o \cos\theta]$ and $\mathbf{E} = [0, E_y = V_o B_o \cos\theta, 0]$. Here θ is the angle with respect the shock surface which is related to the value of the cross-shock component of the magnetic field. The normalization used describes the time in units of the inverse upstream gyrofrequency $\Omega_o = qB_o/mc$, the velocity in the upstream average drift V_o, and distances in the upstream drift gyroradius V_o/Ω_o. Owing to the structure of the electromagnetic forces, equation (7) describes an autonomous (no explicit time dependence on the right-hand side) and conservative (volume preserving, i.e., $\nabla\mathbf{G} = 0$) system. The results are displayed as time series of a phase space coordinate, two-dimensional projections of the phase diagram or as a distribution function versus the initial or final energies.

3.1. Shock-Crossing Ions: Gyrophase Sensitivity

[19] The particles which interact with the electromagnetic inhomogeneous structure and wave turbulence may follow elaborate paths in phase space due to the drifts in the combined self-consistent electric and magnetic fields. In the upstream unperturbed solar wind, in the shock frame, the particles gyrate around the magnetic field and drift due to the motional electric field, and as they encounter additional fields at the vicinity of the structure, they may undergo significant modifications in their phase space trajectories. The diversion of the trajectories due to the inhomogeneity of the electromagnetic fields may depend on the values of their energy, pitch angle, and gyrophase at the shock entry. Therefore the final phase space density of the ions may depend on their energies, and their initial pitch angle and gyrophase distribution. Here we concentrate on the effect of the initial upstream position (which determines the gyrophase) on ion energization.

[20] Figures 4–6 display a subset of the phase space cross sections of representative hydrogen ions with an almost identical initial conditions, differing by a very small

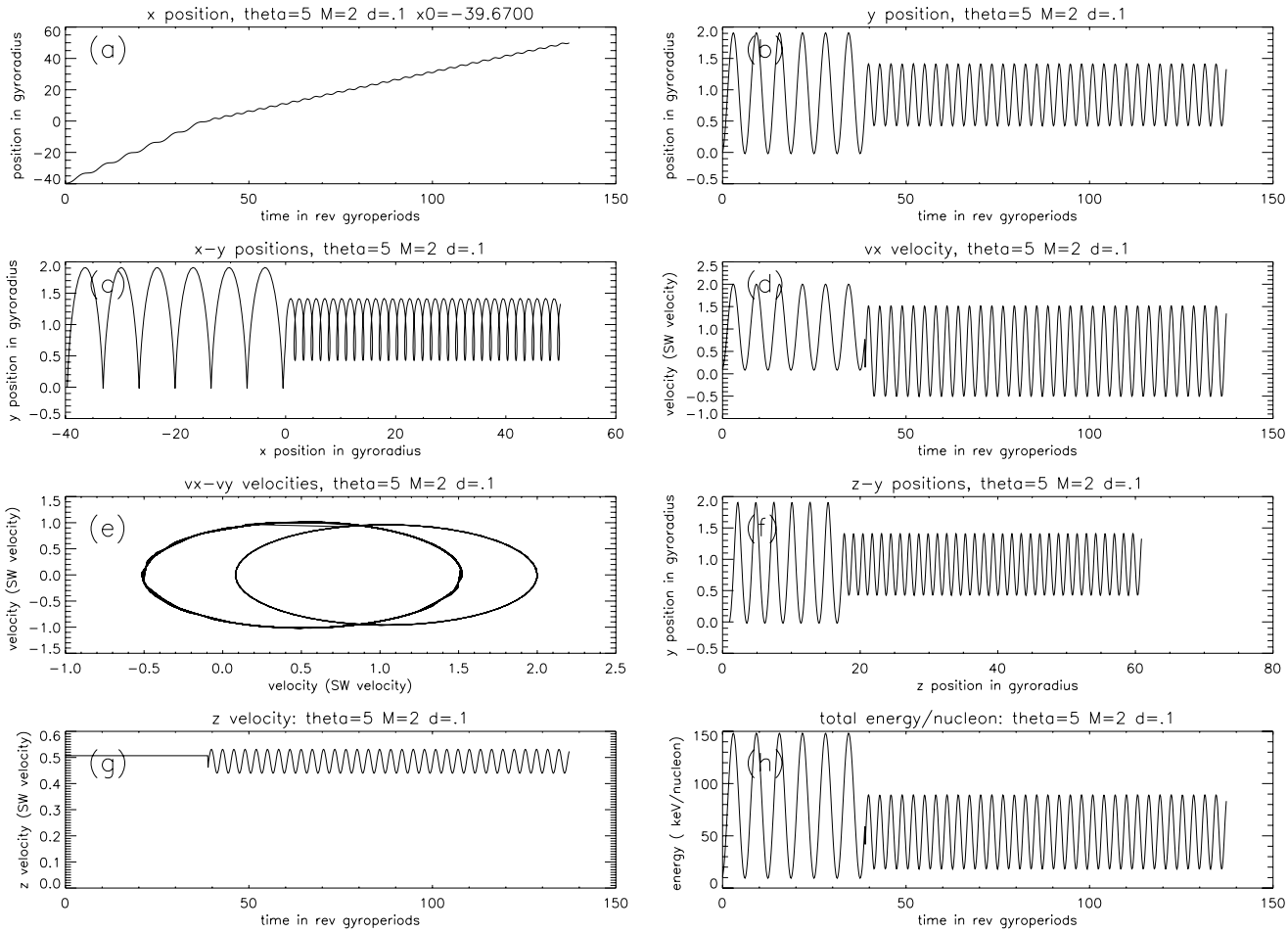

Figure 4. Initial gyrophase effects. Time dependence and phase space cuts for given ion quantities: (a) x(t), (b) y(t), (c) y versus x, (d) $V_x(t)$, (e) V_y versus V_x, (f) z versus y, (g) $V_z(t)$, (h) total kinetic energy (in keV) versus time. The initial values are x = −39.67, y = 0.0, z = 1.0, V_x = 0.1, V_y = 0.2, V_z = 0.5. Position are measured in motional gyroradii, velocities are normalized to the upstream solar wind velocity. Shock parameters: Alfvenic Mach number = 2, plasma β = 0.1, upstream angle between the shock surface and the magnetic field $\theta = 5.0°$, shock width 2δ = 0.1 ion skin depths c/ω_i. The coordinate orientation denotes the shock normal along x, the upstream/downstream magnetic field in the x-z plane and the motional electric field along y. The upstream magnetic field is tilted by 85 degrees off the normal. The ratio of ion gyrofrequency to ion plasma frequency is 0.002.

displacement in their positions (gyrophases). No wave field are imposed. We present three ions with initial x (normalized) positions at an arbitrary time t = 0: x = −39.67 (Figure 4), −39.55 (Figure 5), and −39.25 (Figure 6). One observes that small changes in the initial position may have a very profound effect on the ion trajectory and result in a completely different final location, pitch angle, and energy. In Figure 4 the ion enters the shock around the time $\sim 40\ \Omega_o^{-1}$ (Figure 4a) with a relatively large x velocity (Figure 4d), which can be seen at the intersection of the two curves and the changing topology in the insert (Figure 4e); it encounters the full strength of the cross-field electric field (E_x) and over time much shorter than inverse gyrofrequency is slowed down slightly (Figure 4e) (with an observable clear kink in the $V_x(t)$ trajectory), and traverses the structure without any drift (Figure 4c) along its surface (y direction). As a result, its gyroradius decreases (Figure 4a) as well as the kinetic energy (Figure 4h). In Figure 5 the ion enters the shock with slightly different gyrophase, and smaller x velocity (Figure 5d) on the inner curve of Figure 5e, displaying a stronger kink, such that it reverses its x velocity and therefore starts surfing along the surface in the y direction over a short distance (Figures 5b and 5c), crossing the structure with larger gyroradius (Figure 5a) than on Figure 4 and with approximately adiabatic energy increase (Figure 5h). In Figure 6 the ion enters the shock with a very small x velocity (Figure 6d and 6e) and starts surfing along its surface over large distance parallel to the motional electric field (Figure 6b and 6c), acquiring an energy of 10 MeV. The process is terminated when the cross magnetic field overcomes the electric force. This is the essence of the kinetic process of shock surfing [*Sagdeev*, 1966; *Ohsawa and Sakai*, 1987; *Lee et al.*, 1996; *Zank et al.*, 1996, 2001; *Lipatov et al.*, 1998; *Lipatov and Zank*, 1999; *le Roux et al.*, 2000; *Rice et al.*, 2000], which was applied mainly to the pickup ions. In both last figures the diversion of flow due to B_x is indicated

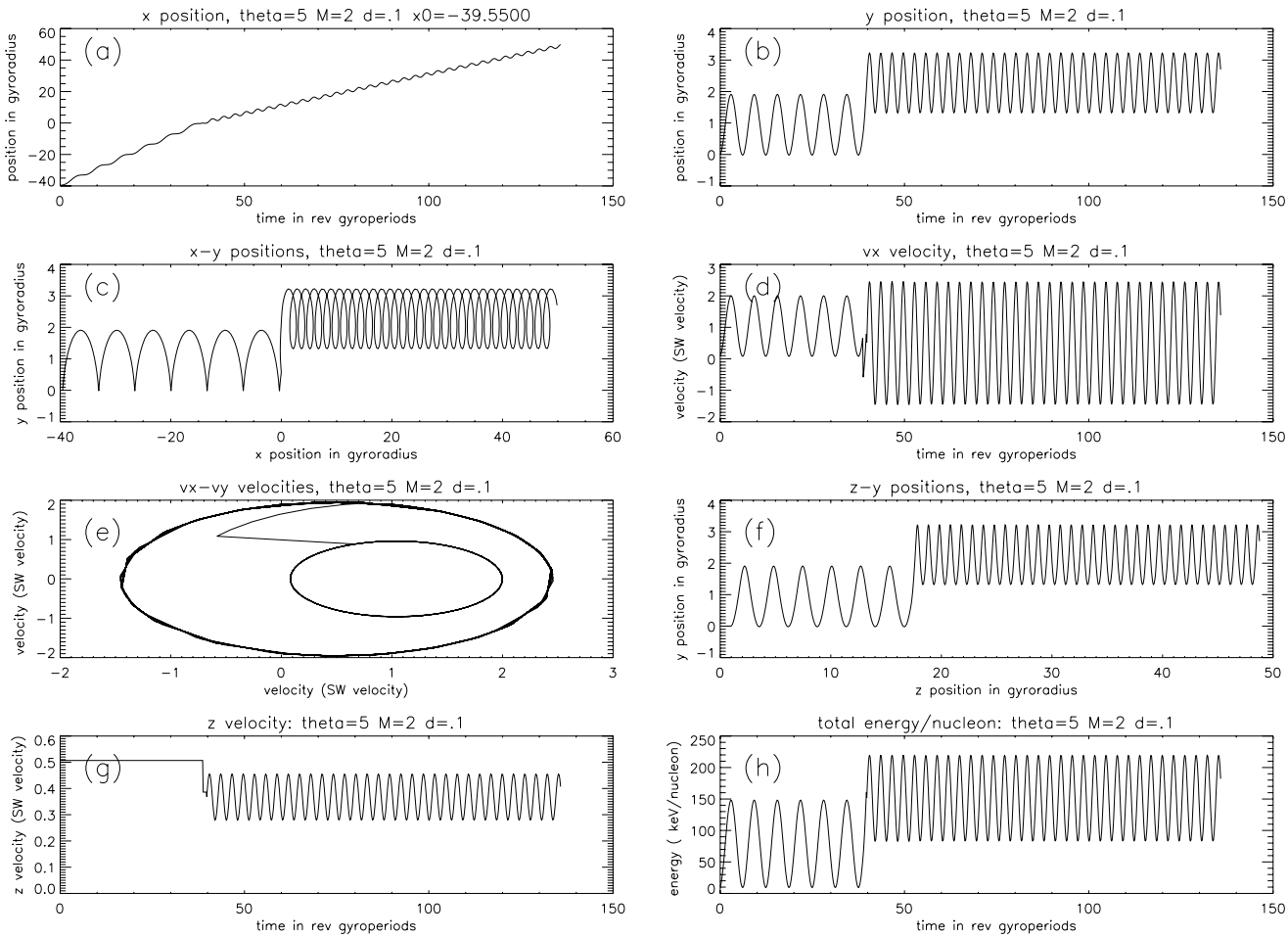

Figure 5. Initial gyrophase effects. Same as Figure 4, with an initial position $x = -39.55$.

by new V_z downstream (Figures 5g and 6g) and motion reversal in z direction. Only a small subset of seed ions enter the shock with a very small V_x and are effectively trapped between the Lorentz force and the cross-shock electrostatic field; as a result they are forced to drift along the y direction where they are accelerated by the motional component of the field (Figures 5–6). For the majority of ions this sensitive condition is not satisfied, hence they are decelerated in the x direction or heated adiabatically and transmitted through the shock (Figures 4–5). Of particular interests are the topological modifications (inserts c and e), indicating important sensitivity to small parameter changes. Ions with lower initial energy or those encountering stronger electric fields may be reflected into the upstream and then encounter the structure at another location with different energy and gyrophase [*Leroy et al.*, 1982; *Leroy and Winske*, 1983]. One can conclude that small deviations in the initial conditions may have a significant effect on ion trajectory. The ion gyrophase dictates the surfing energization. Clearly, the conditions of longer trapping time and more efficient energization are better satisfied for narrow structures.

3.2. Shock-Crossing Ions: Pitch Angle Sensitivity

[21] The sensitivity of particle trajectories to the initial conditions and especially to the value of the normal (x) velocity component during the entry into the shock region may have important implications for ion acceleration by a propagating shock when the flow angle of the plasma changes with respect to the magnetic field. Since the shock propagates through an inhomogeneous interplanetary medium, the orientation of the magnetic field may change while flow stays approximately radial, and the configuration which is determined by the shock normal, plasma flow and magnetic field may assume a variety of possible geometries. Particles which cross a shock may have encountered previously another shock or electromagnetic obstacle which modifies the pitch angle of the interacting ions (equation (3)). Therefore interaction between particles and succession of adjacent shocks may be influenced by the changing directions of the refracted drifts. Additionally, two particles taken from an identical distribution function, with the same energy but different pitch angles encounter the shock with disparate values of the x component velocity (gyrophase) and interact differently with the shock. In contrast to a particle with a small V_x but large V_z which can be slowed down, trapped by the Lorentz and electrostatic forces and start surfing along the shock, the equivalent particle with a large V_x but small V_z has a very small probability to be affected by the combination of the electromagnetic forces and is less likely to be energized by surfing.

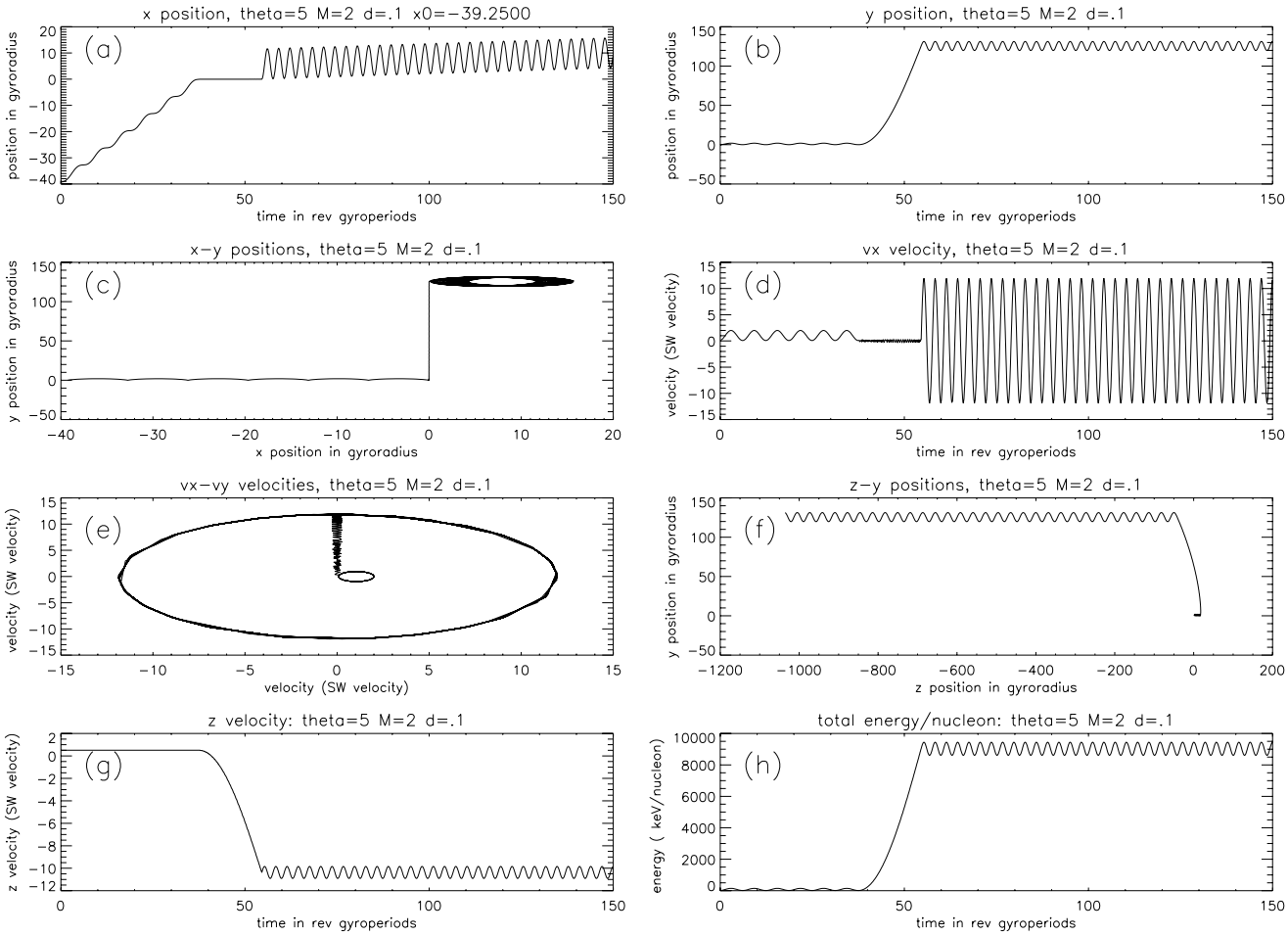

Figure 6. Initial gyrophase effects. Same as Figure 4, with an initial position $x = -39.25$.

[22] Figures 7 and 8 show two particles with identical initial conditions, including the same set of locations and energies, but with interchanged values of V_x and V_z. The upstream parameters are slightly different from Figures 4–6, with a twice broader structure and different magnetic field inclination, to emphasize the generality of the energization process. Similarly to Figure 6, Figure 7 shows a particular ion which was energized via shock surfing, while majority of the ions follow trajectories similar to Figures 4 or 5; in the runs represented by Figure 8 (equal energy but different pitch angle) no energization occurs. One observes that while a subset of particles with initial conditions of Figure 7 may be accelerated up to 0.5 MeV or more, depending on the initial phase space resolution, no particles with the configuration of Figure 8 are significantly energized by the shock. The orientation of the ion drift (pitch angle) affects the gyrophase and shock surfing energization of the thermal population. This result may contribute to the recent study which confirmed the effect of shock geometry on the resulting ion acceleration [*Tylka et al.*, 2005]. In the absence of shock surfing it may also help in modeling the rogue SEP events which were analyzed via changing focusing lengths [*Kallenrode and Cliver*, 2001b].

3.3. Distribution Functions of the Interacting Ions

[23] For relatively narrow structures, with a width of a fraction of the ion skin depth, the effects described in previous subsections show sensitivity to deviations in the initial phase space coordinates (gyrophase and pitch angle), hence a good resolution in this variable is required. In all of the simulations a resolution of 0.0025 or higher in the x coordinate (normalized to the motional gyroradius (V_o/Ω_o)) and 0.1 V_o in velocities is employed, in order to obtain a good description for the energized particles. Therefore to obtain a reasonably accurate distribution function of ions interacting with a relatively narrow structure, one is required to employ a large number of ions with a sufficient resolution in the x position and velocity. For each value of energies (velocities) we follow hundreds of ions with slightly changing initial positions; presentation of the resulting transmitted or reflected trajectories in a format of Figures 4–8 for thousands of ions creates a visually illuminating reconfiguration of the phase space. We repeat the calculations for a variety of energies, pitch angles, and gyrophases, and accumulate the final phase space positions to form an energy distribution. It is clear that only a small subset of particles is accelerated via shock surfing; however, the importance of this process is in the availability of a direct, local acceleration mechanism for the thermal population. Explicit integration of particle trajectories is the most direct evidence of the plausibility of a thermal source for the seed population. These results, while averaged over the full initial phase space may render a realistic distribution function as it emerges from the chosen seed population, in its

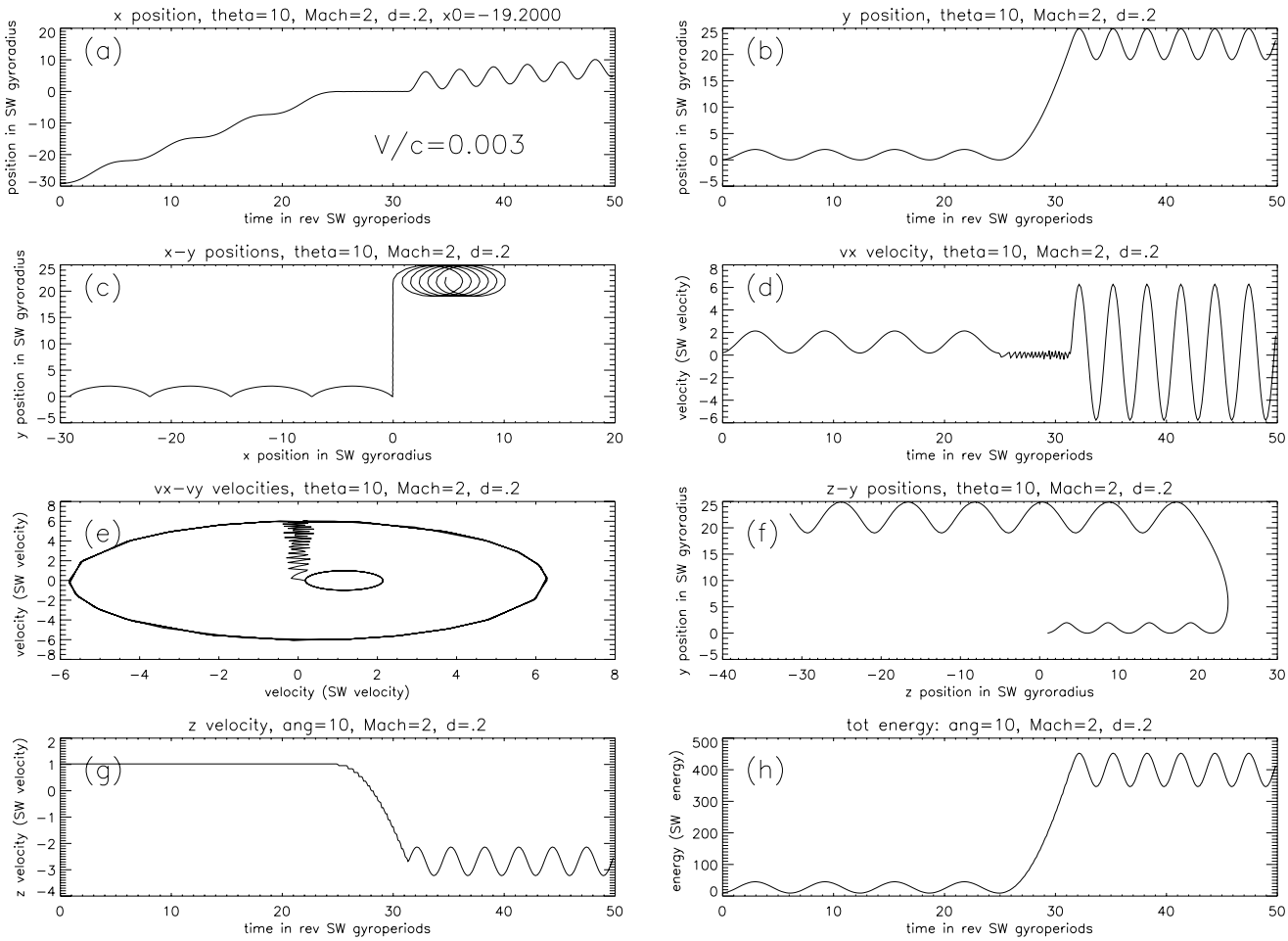

Figure 7. Geometrical comparison. Trajectory of shock-energized ion. Initial values: x = −19.2, y = 0.0, z = 1.0, V_x = 0.2, V_y = 0.2, V_z = 1.0. Shock parameters: Mach number = 2, plasma β = 0.1, θ = 10°, 2δ = 0.2 ion skin depths.

functional shape and in the absolute value of the density of the accelerated particles. The ions in the energetic tail of the distribution are the crucial ingredient of the population which may be later trapped in the the quasi-stable orbits of terrestrial magnetic field. Upstream ions which cross the CME shock propagate generally sunward along the heliospheric field lines; since these fields increase toward the Sun, most of the ions will be reflected by the mirror force and those with a favorable connection to the terrestrial magnetosphere may be trapped in the terrestrial orbits.

[24] Figure 9 shows the distribution functions averaged over 50,000 H ions which enter a Mach-2 shock with a width of 0.1 ion skin depth (approximately four electron skin depths). The structure propagates with a velocity of V = 0.005 c; the ions are distributed initially over 250 *x* locations, covering a distance of one motional gyroradius, along with 20 values of V_x and 10 values of V_z in the range of 0.1−1.0*V*, i.e., in the shock frame they approximately describe a spread of ∼60 keV. The seed population is depicted by asterisks, while the emerging distribution is illustrated by diamonds. One observes formation of an energetic tail with a cutoff around 10 MeV. This result emphasizes the availability of energization mechanism for thermal populations to high energies at small Mach number shocks, without a need of a turbulent medium which is required for a Fermi diffusive scattering.

3.4. Shock Energization of Trace Elements

[25] During active solar periods, when coronal magnetic activity and the number of impulsive flares increase substantially, the Sun emits intermittently ions with abundances which differ from the standard coronal populations by a significant enhancement of particular elements and isotopes states [e.g., *Reames et al.*, 1994]; they include mainly the ^{3}He isotopes, elements around Fe with higher charge states and set of ultra heavy elements at the Xe and Kr groups [*Reames*, 2000; *Mason et al.*, 2004]. At some periods these trace ions fill a significant part of the heliosphere [e.g., *Mason et al.*, 2002]. Together with the solar wind elements and interstellar or interplanetary dust pickup ions, they may serve as a seed population for an additional energization process in the propagating shocks. ACE satellite provided evidence that the seed population for shock acceleration includes suprathermal heavy ions [*Desai et al.*, 2003, 2004]. The question of energization of these trace heavy ions to high energies is of importance since Fe or Kr ion with an equivalent energy/nucleon to a hydrogen ion, is more than 50 times more energetic, i.e., energization of 1−10 MeV/

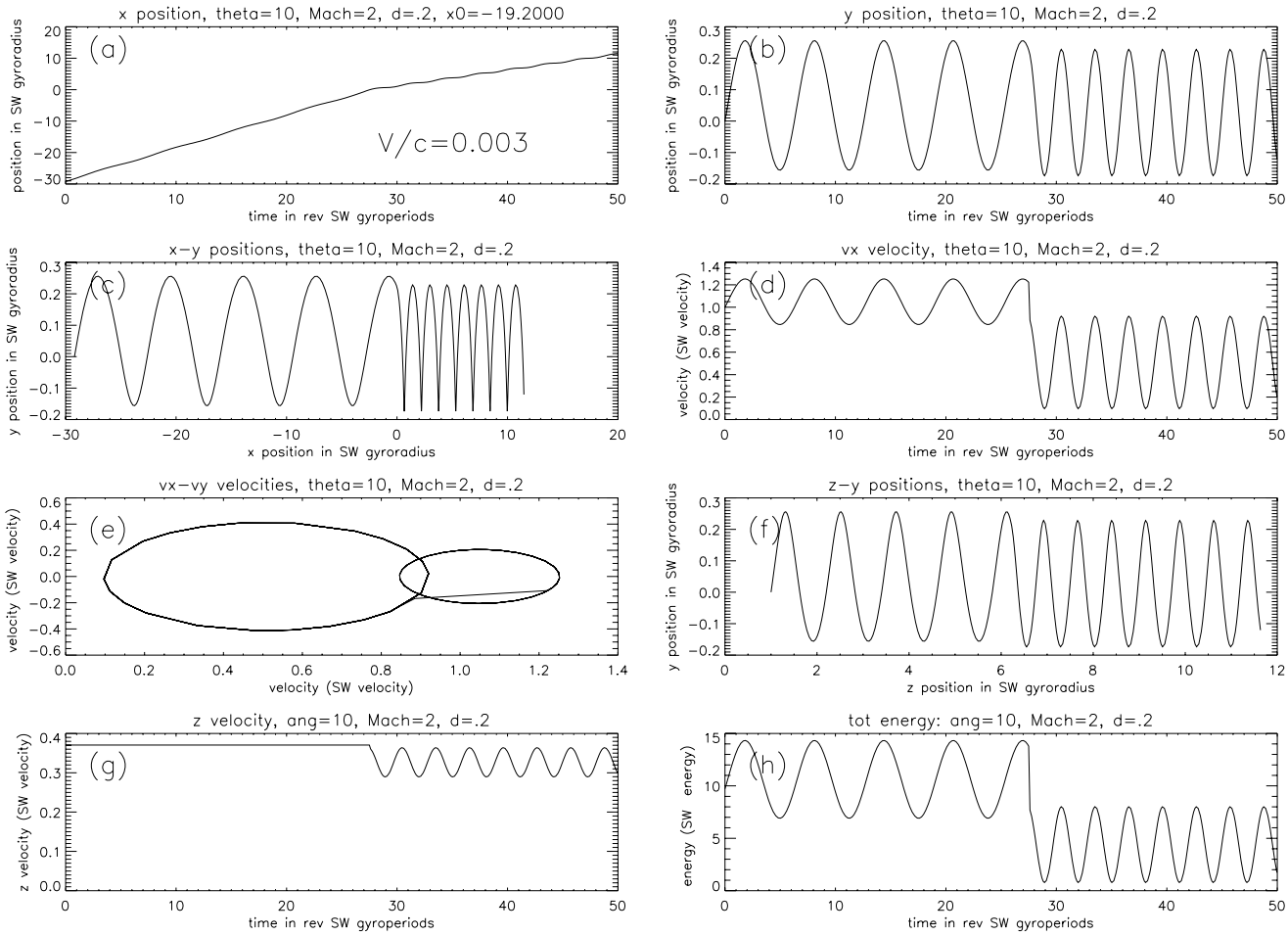

Figure 8. Geometrical comparison. Typical trajectory. Same as Figure 7 with exchanged velocities. Initial values: x = −19.2, y = 0.0, z = 1.0, V_x = 1.0, V_y = 0.2, V_z = 0.2.

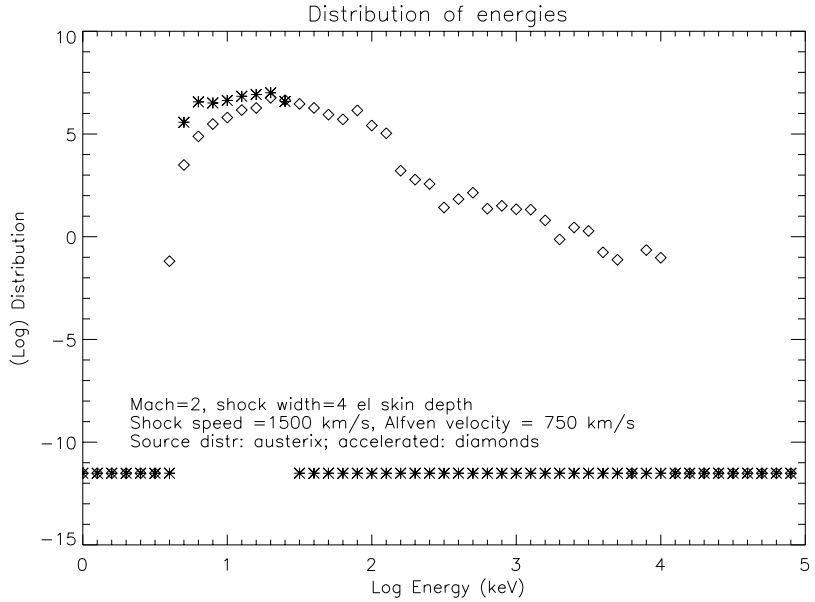

Figure 9. Distribution function of 50,000 hydrogen ions averaged over the initial distribution consisting of a seed population with 6–60 keV (in the shock frame). Shock width 0.1 c/ω_i, ion gyro/plasma ratio = 0.002. Linear energy interpolation was performed a posteriori.

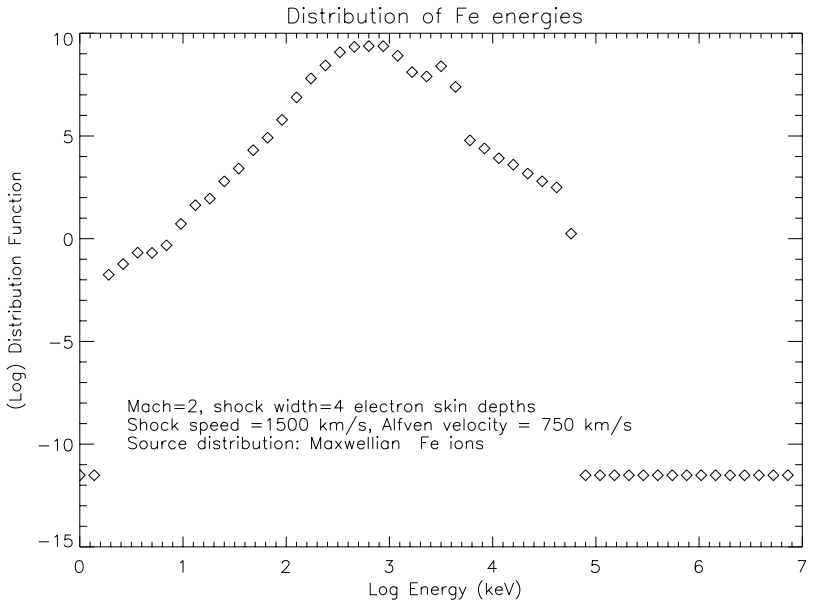

Figure 10. Distribution function of 100,000 $^{20}Fe^{56}$ ions averaged over the initial distribution of 250 locations in x and velocity spread with 40 (10) values of V_x (V_z) in the range of 0.1–1.0 V_o. V_o = 0.005 c; shock width 0.1 c/ω_i.

nucleon is equivalent to ~0.1–1 GeV for heavy ions. Fe ions were observed intermittently in trapped radiation belt orbits at distances of 2–4 Earth radii after a passage of interplanetary shock [e.g., *Lorentzen et al.*, 2002].

[26] Observations of rare (Fe) ions during impulsive solar events indicate that coronal energization applies to energies from tens of Mev/nuc down to 10 keV/nuc [e.g., *Mason et al.*, 2002]. Models of coronal resonant processes are able to energize selective elements with high charge states from the coronal temperature of 100 eV (2 eV/nuc for Fe) to energies at the range of 10 keV/nuc to more than 1 MeV/nuc [e.g., *Roth*, 2001]. Fe ion with an energy of 10 keV/nuc has velocity (in absolute value) of the order of the fast propagating shock (1000 km/s), allowing an effective interaction with the shock. A small subset of gyrating Fe ions with higher energies and appropriate gyrophases will be slowed down at the shock encounter and trapped into shock-surfing. Therefore the phase space of these ions, which may interact with the shock, is not negligible. However, other minor ions (C, N, O) which are not energized/enriched in the coronal process (impulsive flare) are transmitted through the supersonic shock without surfing; the resulting enhanced ratio of energetic Fe/O due to surfing consists of Fe ions with a higher charge state.

[27] In order to represent the interaction of a heavy trace element with the propagating shock we employ the same procedure as described in previous sections for the hydrogen ions. We chose the representative trace element as $^{20}Fe^{56}$ ion, since it is one of the most abundant ions preenergized on flaring coronal lines by a possible wave resonant processes [e.g., *Roth and Temerin*, 1997] and emitted into the heliosphere. The trajectories of $^{20}Fe^{56}$ ions exhibit behavior similar to H ions as shown on Figures 4–6, with a tiny minority being trapped along the shock surface. Figure 10 shows the final distribution functions averaged over 100,000 Fe ions which enter a Mach-2 shock with a width of four electron skin depths. The shock propagates with a velocity of V_o = 0.005 c; the ions are initially distributed over 250 locations in x, covering a distance of one gyroradius, along with 40 (10) values of V_x (V_z) in the range of 0.1–1.0 V_o.

[28] One may observe the formation of an energetic tail reaching 0.1 GeV (20 MeV/nuc). We conclude that minority ions, exemplified here by Fe, which were emitted prior to the emergence of the CME into the heliosphere, presumably due to impulsive solar flares, can be accelerated by an appropriate configuration to high energies even without the diffusive shock acceleration mechanism. In the presence of the turbulence the diffusive acceleration may extend the energetic tail to higher energies.

3.5. Diffusive Contribution to Ion Acceleration

[29] The self-consistent narrow electromagnetic structure forms a natural configuration enabling ion acceleration directly from the thermal seed populations. However, formation of an electromagnetic structure with a small width of a fraction of ion skin depth requires particular conditions with a continuous external drive: in the heliospheric context it can happen in the initial stage of CME formation due to a merging of two or more intense perturbations or when a large velocity ratio between the interacting streams in the solar wind flow is satisfied. As the shock evolves it tends to relax its large inhomogeneities as well as to slow down due to drag forces and, although the skin depth increases with heliocentric distance, the (normalized) width of the shock will generally increase. Additionally, as the shock propagates into increasing heliocentric distances the local Mach number increases and the flow becomes more turbulent. The detailed evolution of the shock is beyond the scope of this paper [*Zank et al.*, 2000; *Rice et al.*, 2003]; however, the turbulent spectrum of waves is an inherent part of the shock. Therefore in order to simulate the additional turbulence on

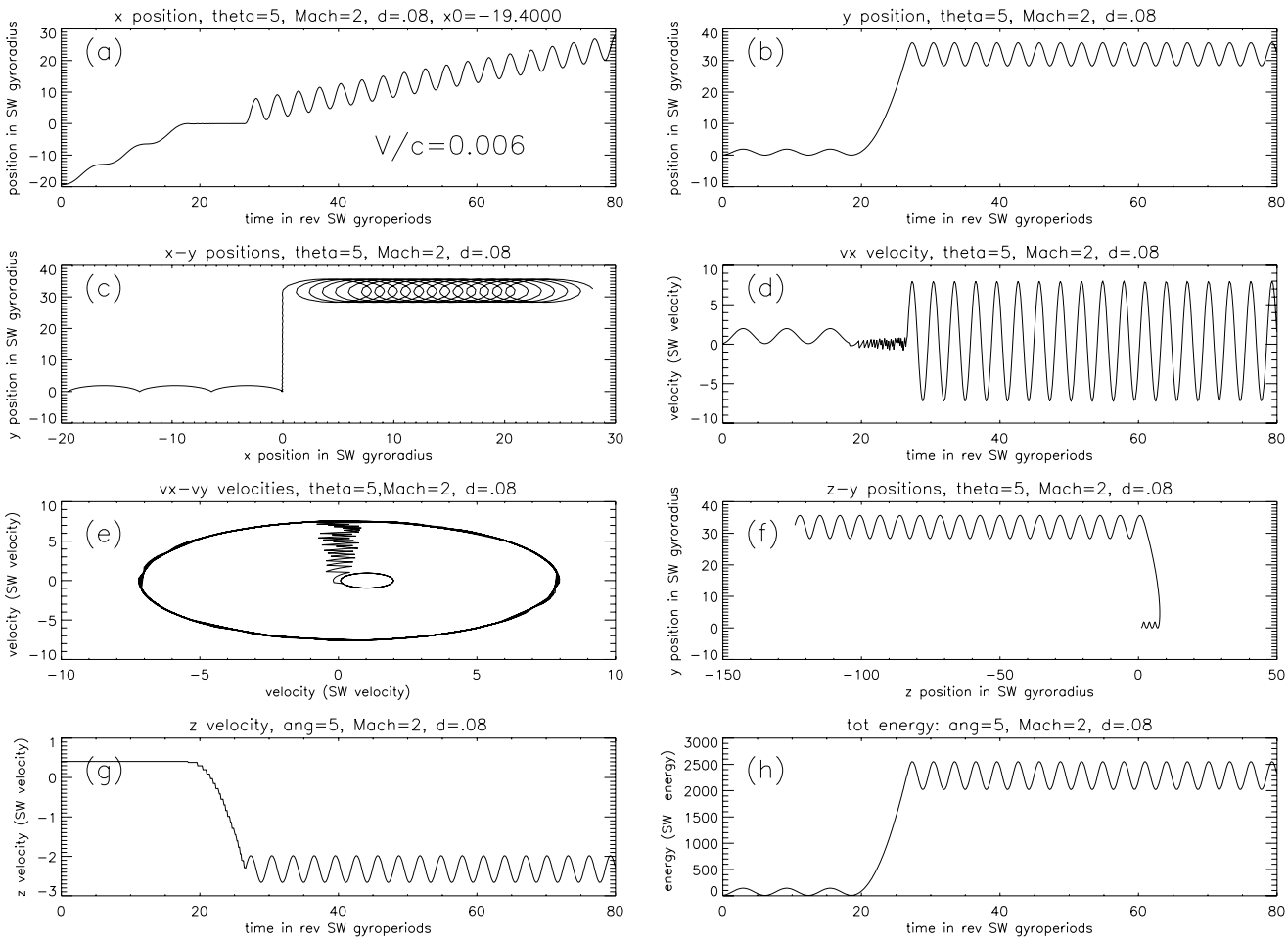

Figure 11. Time-dependence and phase space cuts without turbulence. Shock width 0.08 c/ω_i, ion gyro/plasma ratio = 0.0015. V/c = 0.006.

particle phase space motion, we impose in the stationary shock model of section II a spectrum of Alfven waves, as described at the end of that section. The main parameters which determine the intensity of the waves are the ratio of wave to the ambient energy density given in the range σ_t = 0.4–0.8, the extent of the spatial turbulence given by the normalized $\gamma_L/(c/\omega_i)$ = 50 (10) downstream (upstream, due to this less turbulent region), and by the wave number cutoff Λ/ρ = 100.

[30] Direct comparison of many pairs of runs with and without turbulent wave activity and inspection of trajectories of ions in comparable cases indicate that the main significant deviations in final trajectories occur for particles which got energized via surfing and then undergo shock-drifting with multiple shock crossings. We note that for a vast majority of ions the effect of the waves is small. Figures 11 and 12 show projections and time dependences with identical initial conditions (Figures 11a and 12a) without and (Figures 11b and 12b) with the inclusion of wave spectrum, respectively, for two trajectories of ions where the effect of the turbulence is significant. The turbulence consists of 200 waves with intense power of σ_t = 0.8. The other parameters are: Ω_i/ω_i = 0.0015, 2δ = 0.1 c/ω_i and V/c = 0.006. In the absence of waves the ion is trapped at the entry into the shock and its phase space path is similar to Figure 6 with an energization of 2.5 MeV. In the presence of the turbulence one observes that the ion is first accelerated surfing along the shock (its x position hardly changes); after ejection from the shock downstream it interacts with the waves and gets scattered, eventually being reflected and brought back to the shock, performing multiple crossings (Figures 12a and 12c) and drifting along the shock (its x,y positions describe distorted gyration), with a slow average increase in energy (Figure 12h). In this example the shock-drift process is more prominent than the diffusive acceleration. The final energy for this ion is 6 times higher than the one without the turbulent interaction (Figure 11). We note that some ions may be derailed from shock surfing by the waves and their final energy will be decreased, however generally, once preenergization has been accomplished, the energetic ion tail will be enhanced due to the waves.

[31] Figure 13 shows the final energy distribution function averaged over 50000 ions with the inclusion of waves. Although here we have chosen a broader shock width with 2δ = 0.2c/ω_i (decreasing the energization due to shock surfing) and smaller intensity waves with σ_t = 0.4, one finds that the tail of the distribution function extends above 10 MeV. We conclude that the surfing mechanism becomes the most important energization mechanism in the absence

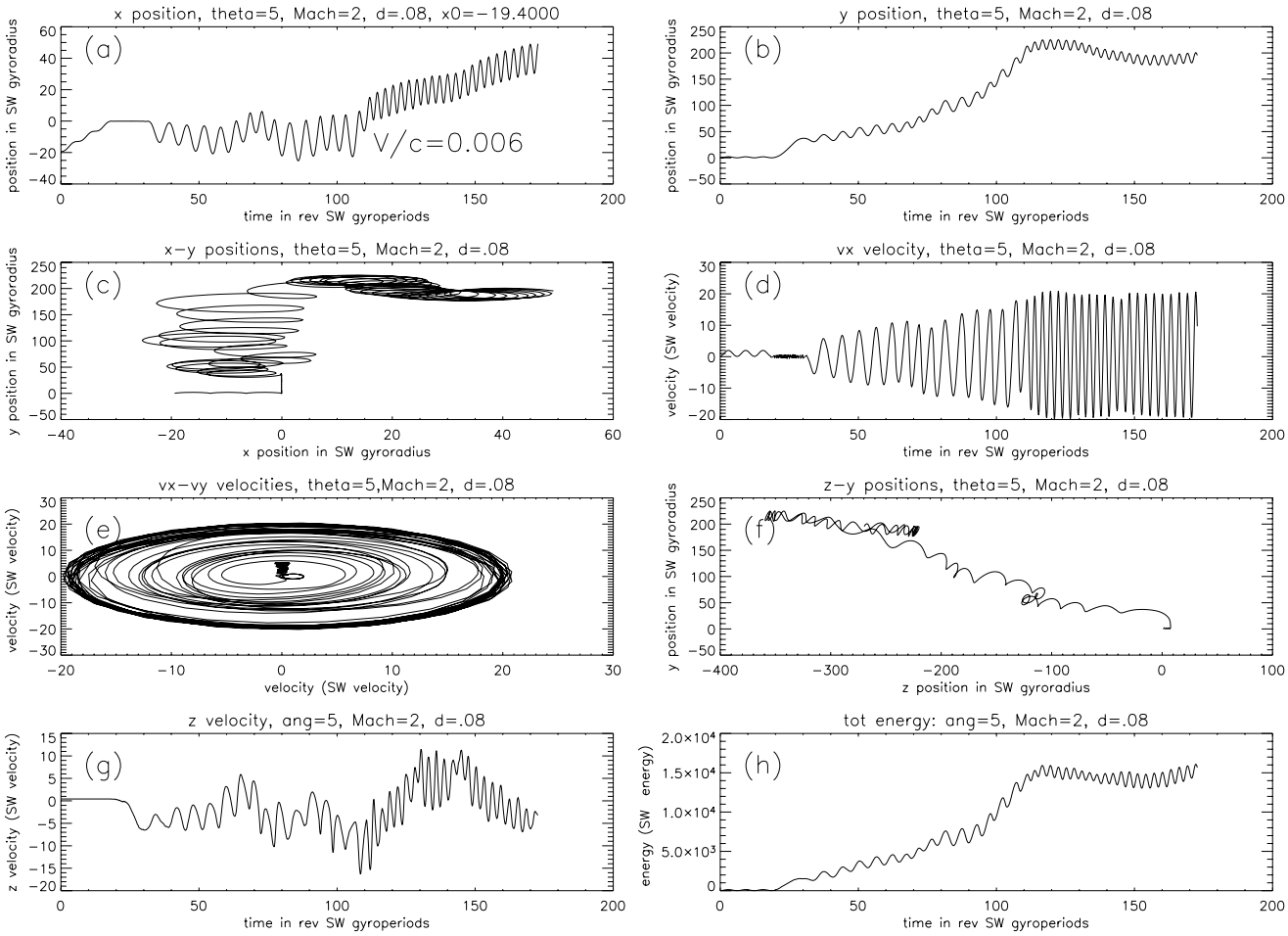

Figure 12. Same as Figure 11, with an imposed turbulence: $\sigma_t = 0.8$.

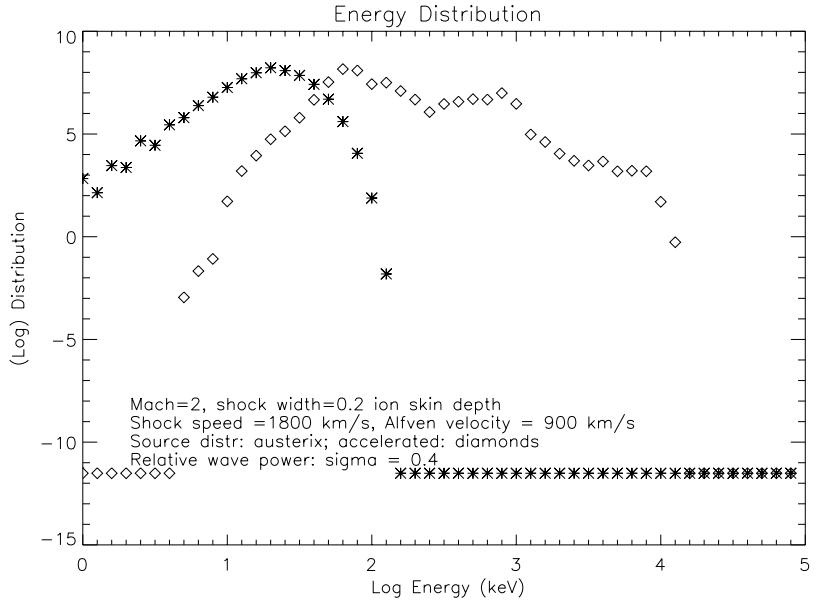

Figure 13. Distribution function of 50,000 hydrogen ions averaged over the initial distribution consisting of a seed population with 6–60 keV, in a presence of waves. Wave power (normalized) σ_t = 0.4, shock width 0.2 c/ω_i, ion gyro/plasma ratio = 0.002, V/c = 0.006.

of a substantial turbulence, and a prerequisite condition for an initiation of the diffusive shock acceleration process.

4. Discussion and Summary

[32] The Sun ejects into the heliosphere minute amount of its mass, energy, and due to the magnetic field embedded in the ejected plasma, magnetic helicity, in the form of solar wind and CMEs. Although the amount of the ejected quantities is minuscule in comparison with the total solar content, they may have an impact on the evolution of the solar magnetic field structure (possible accumulation of CMEs helicities over the solar cycle may contribute to the reversal in solar magnetic polarity), on the formation of very energetic ion fluxes (creating hazard to human exploration of space) and on the intense perturbations to the terrestrial magnetic field (which may enhance the fluxes of relativistic radiation belt electrons with serious implications for the functionality of human technology). It is assumed generally that shock-energized particles have a very small impact on the evolution of the heliospheric shocks because their pressure is insufficient to modify the shock structure (although the most intense shocks, similarly to the 20 January 2005, as well as galactic shocks, may not satisfy this condition). However, in the same way as the CME may be used as tracers of phenomena occurring below the solar atmosphere, energetic particles become effectively early messengers transmitting information on processes which happen along the trajectory of the propagating shock. Owing to the uniqueness of the interaction between the shock, the ambient plasma and the seed population, energetic tail may contribute to our understanding of the propagating shock characteristics.

[33] The CMEs are emitted due to a major relaxation of the stressed coronal field; they propagate supersonically with respect to the solar wind plasma and carry a shock wave ahead of their propagation front. The energetic particles which stream away from the shock interact with the background plasma, forming in its vicinity a turbulent Alfvenic region. The CMEs are formed mainly during magnetically active solar periods, producing intense and direct effects on the terrestrial magnetosphere. Some of the resulting magnetic modifications reduce remarkably the terrestrial ring current, initiating the long-term magnetic storms, while others trigger an abrupt impulse on the terrestrial field causing a storm sudden commencement.

[34] Time profiles of heliospheric ion count rate intensities often indicate formation of very intense fluxes of energetic ions in relative proximity to the Sun, where even for the fast propagating shocks the Alfvenic Mach number and the turbulence levels are low. Hence the value of a high Mach number with an enhanced level of turbulence are not always the crucial factor for an effective energization, and formation of these fluxes creates dilemma regarding the acceleration mechanism. The shock satisfies a set of conservation laws which connect the variables on both the upstream and downstream sides; however, the thickness of the magnetic ramp is not determined by these conservation laws; it evolves self-consistently due to the dynamic interaction with the plasma. Therefore one of the plausible configurations which is able to energize a subset of ions involves a narrow sheath or substructure, formed due to merging of multiple CME perturbations with a rotation of the magnetic field and enhanced cross-shock electric field. This combination of fields may ''trap'' some ions along the shock surface and energize them due to the motional electric field.

[35] Measurements of the ramp thickness raise an important question relevant to the present analysis. Most observations at the Earth's bow shock [*Scudder et al.*, 1986; *Bale et al.*, 2003] at high Mach number and simulations [*Leroy et al.*, 1982; *Quest*, 1986] indicate ramp thickness of the order of hydrogen gyroradii; *Lever et al.* [2001] emphasized the efficiency of shock surfing for a sufficiently narrow ramp where the electrostatic cross-shock amplitude, which was derived from hybrid simulations, decreased with an increasing Mach number, while *Bale et al.* [2003] showed experimentally that the shock width covers the range of 0.25–5.0 ion skin depths with a peak at $0.5c/\omega_i$, and the ion inertial scaling increases approximately linearly with the Mach number. In contrast to the Mach number values at the bow shock, the interplanetary shocks slow down significantly during their propagation to 1 AU; the spread in their Mach numbers indicates that most of these shocks have $M_A = 1.5–5$, with an extended tail reaching $M_A = 15$. The very fast CMEs which form shocks in the solar vicinity and propagate along path of decreasing Alfven velocity, belong to those at the tail of the observed distribution. Extrapolating the bow-shock finding to the low-Mach propagating shocks at 1 AU and beyond (CME and CIR) one may argue that these quasi-stable structures with widths of the order of ion gyroradius may allow some surfing, however their lower speed limits the energization of the ion tail; the pickup ions become then the most favorable source for the seed population. The narrow substructures which we are concerned with result due to interaction of multiple ''sympathetic'' or homologous CMEs which are emitted from the corona in short time intervals and high speed. The resulting electromagnetic reconfiguration may result in a formation of much narrower substructures which favor ion surfing and formation of energetic tail in the ion distribution.

[36] Although CME shocks energize solar wind plasma with coronal abundances, intermittent observations of enhanced fluxes of rare elements, mainly Fe and ^{3}He, in correlation with propagating shocks indicate that the seed population was contaminated by the minority elements. The high charge states of the heavy elements, which are significantly higher than for similar SW ions, indicate a flare source. Among the heavy elements the impulsive flares enrich mainly high charge states of the Fe group, in contrast to other minor ions (C, N, O) which are not energized in the coronal process. The number of impulsive events increases significantly during active solar periods (1000/year), seeding the population for the more rare large SEP events (10/year). Therefore minority elements which were ejected from the corona become natural seed candidates for an additional shock energization. Among the rare elements, shock surfing is more easily accessible to ions which were preenergized by coronal processes; hence their interaction with a CME shock which emerges from the Sun with a low Mach number results in a strongly enhanced energetic Fe/O ratio and high Fe charge state. Since shock surfing is very sensitive to the preenergization of the heavy elements, this

ratio and the charge states may become strong indicators to the importance of the surfing mechanism.

[37] We conjecture that shocks which are formed at the leading edge of CME become the initial intense accelerators of energetic particles. Particularly, close to the initiation site of the CME, at low Mach values, formation of a narrow electromagnetic structures becomes plausible due to merging of multiple shocks which propagate with different speeds. The resulting substructures sustain a configuration of narrow sheaths with strong magnetic field gradients, energizing the ions via shock surfing in the low Alfven Mach numbers and low turbulence level, while plowing through the background plasma. As the shock propagates away from the Sun into the interplanetary space, its width increases in units of skin depths and its narrow substructures widen and merge, decreasing the efficiency of shock surfing; however, as the increasing Alfven Mach number with heliocentric distance enhances the turbulence around the shock, the diffusive shock acceleration (first-order Fermi mechanism) becomes the main acceleration process. Therefore it is plausible that the existence of the first sharp peak in intensity of energetic ions at few solar radii is related to the formation of a narrow structure in the emerging shock.

[38] The CME-related shocks as observed by satellites and analyzed in global simulations involve intricate structures, where both the magnetic field and bulk plasma flow display oblique angles with respect to the shock. Therefore two similar shocks with almost identical properties (speed, strength, size) can energize ions differently when the relative configuration between the shock, the magnetic field and the bulk speed is significantly modified. Differences in configuration may include also a propagating structure versus combination of two structures moving in tandem, such that ions which were affected by the first form an energized population which interacts with the adjacent one at different geometrical configuration; the resulting spectrum may vary substantially from the one which emerges due to an interaction with only one structure. These configurations may explain partially the different observations of H and/or Fe ion enhancements for similar shocks.

[39] **Acknowledgments.** This work was supported in part by NASA grants NAG5-11944 and FDNAG5-11733 and by contract BU-GC177029NGA of the STC Program (National Science Foundation) under agreement ATM-0120950. The authors are thankful to Janet Luhmann and Dietmar Krauss-Varban for helpful discussions. I.R. expresses his gratitude to the Max-Planck Institut fur Extraterrestrische Physik in Garching for their hospitality during the last phase of this research.

[40] Shadia Rifai Habbal thanks Robert B. Decker and another referee for their assistance in evaluating this paper.

References

Axford, W. I. (1981), Acceleration of cosmic rays by shock waves, *Proc. Int. Cosmic Ray Conf.*, *12*, 155.

Bale, S. D., F. S. Mozer, and T. S. Horbury (2003), Density-transition scale at quasiperpendicular collisionless shocks, *Phys. Rev. Lett.*, *91*(26), 5004.

Balikhin, M., and M. Gedalin (1994), Kinematic mechanism of electron heating in shocks: Theory vs observations, *Geophys. Res. Lett.*, *21*, 841.

Ball, L., and D. Galloway (1998), Electron heating by the cross-shock electric potential, *J. Geophys. Res.*, *103*, 17,455.

Blake, J. B., W. A. Kolasinski, R. W. Filius, and E. G. Mullen (1992), Injection of electrons and protons with energies of tens of MeV into L less than 3 on 24 March 1991, *Geophys. Res. Lett.*, *19*, 821.

Blandford, R., and D. Eichler (1987), Particle acceleration at astrophysical shocks—A theory of cosmic-ray origin, *Phys. Rep.*, *154*, 1.

Cheng, J., C. Fang, P. Chen, and M. Ding (2005), Two sympathetic homologous CMEs on 2002 May 22, *Chin. J. Astron. Astrophys*, *5*, 265.

Desai, M. I., G. M. Mason, J. E. Mazur, J. R. Dwyer, R. E. Gold, S. M. Krimigis, S. W. Smith, and R. M. Skoug (2003), Evidence for a suprathermal seed population of heavy ions accelerated by interplanetary shocks near 1 AU, *Astrophys. J.*, *588*, 1149.

Desai, M. I., et al. (2004), Spectral properties of heavy ions associated with the passage of interplanetary shocks at 1 AU, *Astrophys. J.*, *611*, 1156.

Drury, L. O. (1983), An introduction to the theory of diffusive shock acceleration of energetic particles in tenuous plasmas, *Rep. Progr, Phys.*, *46*, 973.

Duffy, P., L. O. Drury, and H. Voelk (1994), Cosmic ray hydrodynamics at shock fronts, *Astron. Astrophys.*, *291*, 613.

Eichler, D. (1984), On the theory of cosmic-ray-mediated shocks with variable compression ratio, *Astrophys. J.*, *277*, 429.

Ellison, D. C., and S. P. Reynolds (1991), A determination of relativistic shock jump conditions using Monte Carlo techniques, *Astrophys. J.*, *378*, 214.

Fisk, L. A., and M. A. Lee (1980), Shock acceleration of energetic particles in corotating interaction regions in the solar wind, *Astrophys. J.*, *237*, 620.

Gedalin, M., K. Gedalin, M. Balikhin, and V. Krasnosselskikh (1995), Demagnetization of electrons in the electromagnetic field structure, typical for quasi-perpendicular collisionless shock front, *J. Geophys. Res.*, *100*, 9481.

Giacalone, J., and D. C. Ellison (2000), Three-dimensional numerical simulations of particle injection and acceleration at quasi-perpendicular shocks, *J. Geophys. Res.*, *105*, 12,541.

Gloeckler, G., J. Geiss, L. A. Fisk, N. A. Schwadron, and T. H. Zurbuchen (2000), Elemental composition of the inner source pickup ions, *J. Geophys. Res.*, *105*, 7459.

Goldreich, P., and H. Sridhar (1995), Toward a theory of interstellar turbulence: Strong alfvenic turbulence, *Astrophys. J.*, *438*, 763.

Gopalswamy, N., S. Yashiro, G. Michalek, M. L. Keiser, R. A. Howard, D. V. Reames, R. Leske, and T. T. von Rosenvinge (2002), Interacting coronal mass ejections and solar energetic particles, *Astrophys. J.*, *572*, L103.

Hudson, M. K., V. A. Marchenko, I. Roth, M. Temerin, J. Blake, and S. Gussenhoven (1998), Radiation belt formation during storm sudden commencements and loss during main phase, *Adv Space Res.*, *21*, 597.

Hundhausen, A. J., and J. T. Gosling (1976), Solar wind structure at large heliocentric distances: An interpretation of Pioneer 10 observations, *J. Geophys. Res.*, *81*, 1436.

Kahler, S. W. (1992), Solar flares and coronal mass ejections, *Annu. Rev. Astron. Astrophys.*, *30*, 113.

Kallenrode, M. B., and E. W. Cliver (2001a), Rogue SEP events: Observational aspects, *Proc. Int. Conf. Cosmic Rays 27th*, 3314.

Kallenrode, M. B., and E. W. Cliver (2001b), Rogue SEP events: Modeling, *Proc. Int. Conf. Cosmic Rays 27th*, 3318.

Krymsky, G. S. (1977), A regular mechanism for accelerating charged particles at the shock front, *Dokl. Akad. Nauk. SSSR*, *234*, 1306.

Lee, M. (2005), Coupled hydromagnetic wave excitation and ion acceleration at an evolving coronal/interplanetary shock, *Astrophys. J. Suppl. Ser.*, *158*, 38.

Lee, M. A., V. D. Shapiro, and R. Z. Sagdeev (1996), Pickup ion energization by shock surfing, *J. Geophys. Res.*, *101*, 4777.

Lembege, B., P. Savoini, M. Balikhin, S. Walker, and V. Krasnoselskikh (2003), Demagnetization of transmitted electrons through a quasi-perpendicular collisionless shock, *J. Geophys. Res.*, *108*(A6), 1256, doi:10.1029/2002JA009288.

le Roux, J. A., H. Fichtner, and G. P. Zank (2000), Self-consistent acceleration of multiply reflected pickup ions at a quasi-perpendicular solar wind termination shock: A fluid approach, *J. Geophys. Res.*, *105*, 12,577.

Leroy, M. M., and D. Winske (1983), Backstreaming ions from oblique Earth bow shocks, *Ann. Geophys.*, *1*, 527.

Leroy, M. M., D. Winske, C. C. Goodrich, C. S. Wu, and K. Papadopoulos (1982), The structure of perpendicular bow shocks, *J. Geophys. Res.*, *87*, 5081.

Lever, E. L., K. Quest, and V. D. Shapiro (2001), Shock surfing vs. shock drift acceleration, *Geophys. Res. Lett.*, *28*, 1367.

Lipatov, A. S., and G. P. Zank (1999), Pickup ion acceleration at low-betap perpendicular shocks, *Phys. Rev. Lett.*, *82*(18), 3609.

Lipatov, A. S., G. P. Zank, and H. L. Pauls (1998), The acceleration of pickup ions at shock waves: Test particle-mesh simulations, *J. Geophys. Res.*, *103*, 29,679.

Lorentzen, K. R., J. E. Mazur, M. D. Looper, J. F. Fennell, and J. B. Blake (2002), Multisatellite observations of MeV ion injections during storms, *J. Geophys. Res.*, *107*(A9), 1231, doi:10.1029/2001JA000276.

Mason, G. M., et al. (2002), Spectral properties of He and heavy ions in 3He-rich solar flares, *Astrophys. J.*, *574*, 1039.

Mason, G. M., J. E. Mazur, J. R. Dwyer, J. R. Jokipii, R. E. Gold, and S. M. Krimigis (2004), Abundances of heavy and ultraheavy ions in 3He-rich solar flares, *Astrophys. J.*, *606*, 555.

McDonald, F. B., T. J. Teegarten, J. H. Trainor, T. T. von Rosevinge, and W. R. Webber (1976), The interplanetary acceleration of energetic nucleons, *Astrophys. J.*, *203*, L149.
Mikic, Z., and J. A. Linker (1994), Disruption of coronal magnetic field arcades, *Astrophys. J.*, *430*, 898.
Ohsawa, Y., and J. Sakai (1987), Nonstochastic prompt proton acceleration by fast magnetosonic shocks in the solar plasma, *Astrophys. J.*, *313*, 440.
Papadopoulos, D. (1985), in *Collisional Shocks in the Heliosphere*, *Geophys. Monogr. Ser.*, vol. 34, edited by R. G. Stone and B. T. Tsurutani, p. 59, AGU, Washington, D. C.
Quest, K. (1986), Simulations of high Mach number perpendicular shocks with resistive electrons, *J. Geophys. Res.*, *91*, 8805.
Reames, D. V. (1995), Solar energetic particles: A paradigm shift, *Rev. Geophys.*, *33*, 585.
Reames, D. V. (1999), Particle acceleration at the Sun and in the heliosphere, *Space Sci. Rev.*, *90*, 413.
Reames, D. V. (2000), Abundances of trans-iron elements in solar energetic particle events, *Astrophys. J.*, *540*, L111.
Reames, D. V., and A. J. Tylka (2002), Energetic particle abundances as probes of an interplanetary shock wave, *Astrophys. J.*, *575*, L37.
Reames, D. V., I. J. Richardson, and L. M. Barbier (1991), On the differences in element abundances of energetic ions from corotating events and from large solar events, *Astrophys. J.*, *382*, L43.
Reames, D. V., J. P. Meyer, and T. T. von Rosenvinge (1994), Energetic-particle abundances in impulsive solar flare events, *Astrophys. J. Suppl. Ser.*, *90*, 649.
Reames, D. V., C. K. Ng, and A. J. Tylka (2000), Initial time dependence of abundances in solar energetic particle events, *Astrophys. J.*, *531*, L83.
Reames, D. V., C. K. Ng, and A. J. Tylka (2001), Heavy ion abundances and spectra and the large gradual solar energetic particle event of 2000 July 14, *Astrophys. J.*, *548*, L233.
Rice, W. K. M., G. P. Zank, and J. A. le Roux (2000), An injection mechanism for shock waves of arbitrary obliquity, *Geophys. Res. Lett.*, *27*, 3793.
Rice, W. K. M., G. P. Zank, and G. Li (2003), Particle acceleration and coronal mass ejection driven shocks: Shocks of arbitrary strength, *J. Geophys. Res.*, *108*(A10), 1369, doi:10.1029/2002JA009756.
Roberts, D. A., and M. L. Goldstein (1999), Magnetohydrodynamic turbulence in the solar wind, *Phys. Plasmas*, *6*, 4154.
Roth, I. (2001), Solar coronal acceleration of minority ions and its astrophysical implications, *Proc. Int. Cosmic Ray Conf. 27th*, 3219.
Roth, I., and M. A. Temerin (1997), Enrichment of 3He and heavy ions in impulsive solar flares, *Astrophys. J.*, *477*, 940.
Sagdeev, R. Z. (1966), Cooperative phenomena and shock waves in collision-less plasmas, in *Review of Plasma Physics*, vol. 4, p. 23, Consult. Bur., New York.
Schlickeiser, R. (1989), Cosmic-ray transport and acceleration: Derivation of the kinetic equation and application to cosmic rays in static cold media, *Astrophys. J.*, *336*, 243.
Scholer, M., I. Shinohara, and S. Matsukiyo (2003), Quasi-perpendicular shocks: Length scale of the cross-shock potential, shock reformation, and implication for shock surfing, *J. Geophys. Res.*, *108*(A1), 1014, doi:10.1029/2002JA009515.
Scudder, J. D., T. L. Aggson, A. Mangeney, C. Lacombe, and C. C. Harvey (1986), The resolved layer of a collisionless, high beta, supercritical, quasi-perpendicular shock wave: 2. Dissipative fluid electrodynamics, *J. Geophys. Res.*, *91*, 11,019.
Tidman, D. A., and N. A. Krall (1971), *Shock Waves in Collisionless Plasmas*, Wiley Interscience, Hoboken, N. J.
Tylka, A. J., P. R. Boberg, C. M. Cohen, W. F. Dietrich, M. A. Lee, C. G. Maclennan, G. M. Mason, C. K. Ng, and D. V. Reames (2002), Flare- and shock-accelerated energetic particles in the solar events of 2001 April 14 and 15, *Astrophys. J.*, *581*, L119.
Tylka, A. J., C. M. Cohen, W. F. Dietrich, M. A. Lee, C. G. Maclennan, R. A. Mewaldt, C. K. Ng, and D. V. Reames (2005), Shock geometry, seed populations, and the origin of variable elemental composition at high energies in large gradual solar particle events, *Astrophys. J.*, *625*, 474.
Wang, C., J. Richardson, and L. Burlaga (2001), Propagation of the Bastille Day 2000 CME shock in the outer heliosphere, *Sol. Phys.*, *204*, 411.
Zank, G. P., H. L. Pauls, I. H. Cairns, and G. M. Webb (1996), Interstellar pickup ions and quasi-perpendicular shocks: Implications for the termination shock and interplanetary shocks, *J. Geophys. Res.*, *101*, 457.
Zank, G. P., W. K. M. Rice, and C. C. Wu (2000), Particle acceleration and coronal mass ejection driven shocks: A theoretical model, *J. Geophys. Res.*, *105*, 25,079.
Zank, G. P., W. K. M. Rice, J. A. le Roux, and W. H. Matthaeus (2001), The injection problem for anomalous cosmic rays, *Astrophys. J.*, *556*, 494.
Zilbersher, D., and M. Gedalin (1997), Pickup ion dynamics at the structured quasi-perpendicular shock, *Planet. Space. Sci.*, *45*, 693.

S. D. Bale and I. Roth, Space Sciences Laboratory, University of California, Berkeley, SS21, Berkeley, CA 94720, USA. (ilan@sunspot.ssl.berkeley.edu)